



Integrating pressure sensor control into semi-solid extrusion 3D printing to optimize medicine manufacturing

Eduardo Díaz-Torres^{a,b,c}, Lucía Rodríguez-Pombo^d, Jun Jie Ong^e, Abdul W. Basit^{e,f}, Ana Santoveña-Estévez^{a,b,*}, José B. Fariña^{a,b}, Carmen Alvarez-Lorenzo^d, Alvaro Goyanes^{d,e,f,**}

^a Departamento Ingeniería Química y Tecnología Farmacéutica, Universidad de La Laguna, La Laguna 38200, Spain

^b Instituto Universitario de Enfermedades Tropicales y Salud Pública de Canarias, Universidad de La Laguna, La Laguna 38203, Spain

^c Programa de Doctorado en Ciencias Médicas y Farmacéuticas, Desarrollo y Calidad de Vida, Universidad de La Laguna, 38200 La Laguna, Tenerife, Spain

^d Departamento de Farmacología, Farmacia y Tecnología Farmacéutica, I+D Farma (GI-1645), Facultad de Farmacia, Instituto de Materiales (IMATUS) and Health Research Institute of Santiago de Compostela (IDIS), Universidade de Santiago de Compostela, 15782 Santiago de Compostela, Spain

^e Department of Pharmaceutics, UCL School of Pharmacy, University College London, 29-39 Brunswick Square, London WC1N 1AX, UK

^f Fabrx Ltd, Henwood House, Henwood, Ashford, Kent TN24 8DH, UK

ARTICLE INFO

Keywords:

Ink characterization
Rheology
Printing formulations and drug products
Process analytical technology (PAT)
Paediatric formulations
Direct ink writing of medicines
3D printed pharmaceuticals and drug delivery systems

ABSTRACT

Semi-solid extrusion (SSE) is a three-dimensional printing (3DP) process that involves the extrusion of a gel or paste-like material via a syringe-based printhead to create the desired object. In pharmaceuticals, SSE 3DP has already been used to manufacture formulations for human clinical studies. To further support its clinical adoption, the use of a pressure sensor may provide information on the printability of the feedstock material in situ and under the exact printing conditions for quality control purposes. This study aimed to integrate a pressure sensor in an SSE pharmaceutical 3D printer for both material characterization and as a process analytical technology (PAT) to monitor the printing process. In this study, three materials of different consistency were tested (soft vaseline, gel-like mass and paste-like mass) under 12 different conditions, by changing flow rate, temperature, or nozzle diameter. The use of a pressure sensor allowed, for the first time, the characterization of rheological properties of the inks, which exhibited temperature-dependent, plastic and viscoelastic behaviours. Controlling critical material attributes and 3D printing process parameters may allow a quality by design (QbD) approach to facilitate a high-fidelity 3D printing process critical for the future of personalized medicine.

1. Introduction

Three-dimensional printing (3DP), also called additive manufacturing, is an industry-disrupting manufacturing technology that enables the layer-by-layer fabrication of 3D objects encoded in a digital computer-aided design (CAD) file (Seoane-Viaño et al., 2021a). This technology has been explored in the pharmaceutical field for the personalization of medicines, to avoid dose inaccuracies due to tablet splitting when the correct dosage is not commercially available (Gudeman et al., 2013; Melocchi et al., 2021; Trenfield et al., 2020; Watson et al., 2021).

Semisolid extrusion (SSE) is a 3D printing technology that involves

the extrusion of a gel or paste-like material in sequential layers via a syringe-based printhead on a building plate (Fang et al., 2021; Johansson et al., 2021; Seoane-Viaño et al., 2020a; Seoane-Viaño et al., 2021b; Seoane-Viaño et al., 2020b; Tagami et al., 2021; Vithani et al., 2019; Yan et al., 2020). The preparation of materials for SSE is easy and simple, and a large variety of excipients are available to modulate the final ink properties. These inks may also be loaded with multiple drugs. Moreover, the use of pre-filled and disposable syringes mitigates cross-contamination and facilitates compliance with regulatory requirements, thereby supporting the implementation of SSE in decentralized clinical environments, e.g. in hospitals or community pharmacies. Indeed, the first clinical study using 3DP in a hospital

* Correspondence to: Ana Santoveña-Estévez, Departamento Ingeniería Química y Tecnología Farmacéutica, Universidad de La Laguna, La Laguna 38200, Spain.

** Correspondence to: Alvaro Goyanes, Departamento de Farmacología, Farmacia y Tecnología Farmacéutica, I+D Farma (GI-1645), Facultad de Farmacia, Instituto de Materiales (IMATUS) and Health Research Institute of Santiago de Compostela (IDIS), Universidade de Santiago de Compostela, 15782 Santiago de Compostela, Spain.

E-mail addresses: ansanto@ull.edu.es (A. Santoveña-Estévez), a.goyanes@fabrx.co.uk (A. Goyanes).

<https://doi.org/10.1016/j.ijpx.2022.100133>

Received 11 August 2022; Received in revised form 8 October 2022; Accepted 10 October 2022

Available online 12 October 2022

2590-1567/© 2022 The Authors. Published by Elsevier B.V. This is an open access article under the CC BY-NC-ND license (<http://creativecommons.org/licenses/by-nc-nd/4.0/>).

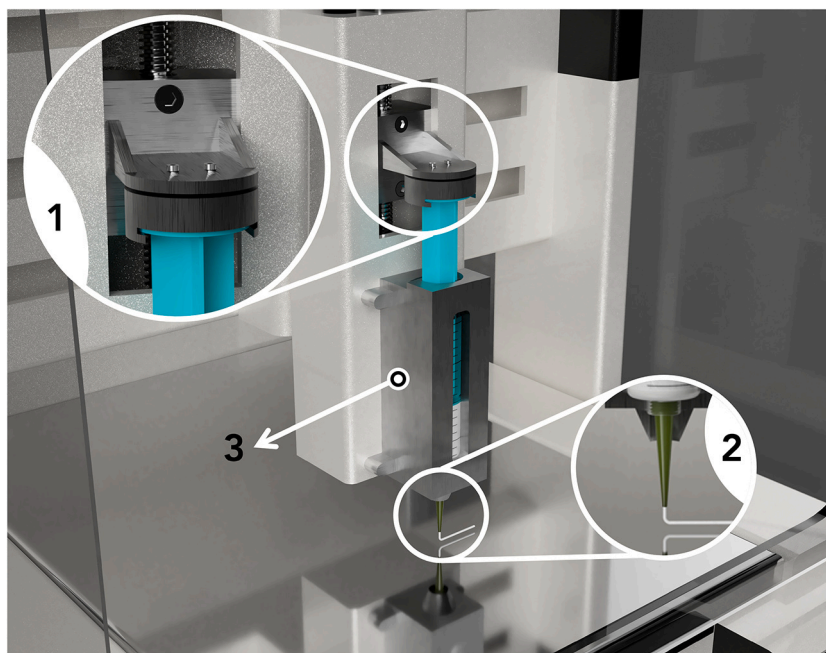


Fig. 1. Schematic view of the M3DIMAKER printing platform equipped with Laguna SSE printhead. 1) Instrumentalized syringe plunger holding system, 2) conical extrusion nozzle (\varnothing 1.60 mm or \varnothing 0.84 mm), and 3) syringe heater system (25 °C, 37 °C or 60 °C).

Table 1

Experimental design for each formulation. The volumetric flow rate is expressed as mm^3 forced through the nozzle per second. The speed at which the syringe plunger descends in mm/s is shown in brackets.

Nozzle inner diameter (mm)	0.84			1.60		
Extrusion flow (mm^3/s)	16.02 (0.05 mm/s)			48.07 (0.15 mm/s)		
Extrusion temperature (°C)	25	37	60	25	37	60

setting to prepare personalized medicines was carried out with an SSE 3D printer. In that study, chewable Printlets™ (3D printed tablets) were administered to children affected by a rare disorder, Maple Syrup Urine Disease (Goyanes et al., 2019).

Despite the advantages of SSE 3DP, a notable challenge lies in finding the correct rheological behaviour of the inks that may provide pharmaceutical products with the appropriate final critical quality attributes (CQA). The rheological behaviour of the materials determines whether a feedstock material candidate has suitable printability characteristics. The extrusion process of the material through the nozzle is normally based on a pneumatic or mechanical systems (Seoane-Viaño et al., 2021a). Pneumatic-based extrusion systems employ pressurized air to compress and extrude the formulation using a valve-free or a valve-based configuration (Ozbolat, 2016; Ozbolat and Hospodiuk, 2016). Mechanical systems (piston or screw) apply mechanical force directly on the top of the syringe to push the material through a nozzle (Ozbolat, 2016). The mechanical approach is simpler than the pneumatic one and more affordable since it does not require an air compressor (Ozbolat, 2016). The piston can also provide greater control over critical extrusion parameters such as the material flow. In addition, the replacement of the syringes can be done in a quick and easy manner, resulting in an overall faster printing process (Seoane-Viaño et al., 2021b).

Although great progress has been made with extrusion systems in the last years, there remains a need for a tool or an instrumented plunger that allows control over the pressure exerted during the printing process. In mechanical SSE 3D printing, pressure applied to the top of the syringe is progressively increased up to a threshold at which material begins to flow through the nozzle. Pressure continues to increase until the desired flow rate is achieved, whereupon the pressure must be kept constant and without large oscillations to assure the quality of the final product. An

increase in the applied pressure would indicate that the nozzle may be clogged. On the other hand, a sudden drop in the pressure may indicate the presence of air inside the syringe or nozzle, resulting in a decrease in the amount of deposited mass (Govender et al., 2021; Rahman and Quodbach, 2021; Seoane-Viaño et al., 2021; Zidan et al., 2018a; Zidan et al., 2018b). Clogging and intermittent material deposition are undesirable as they lead to inconsistent or failed prints. Therefore, a system capable of monitoring the applied pressure would optimize the printing process by establishing correlations between the printing pressure and the quality attributes of the object like weight, size, dose.

Several material properties (e.g. viscosity and printing parameters) and process parameters (e.g. extrusion force or temperature) may affect the printability of the materials (Govender et al., 2021; Zidan et al., 2018a; Zidan et al., 2018b). Materials with low viscosity can be easily extruded, but the final objects may collapse. On the other hand, if the viscosity is high, the material may not flow. The application of a high mechanical force to the ink may improve the flow of the material. Likewise, heating the feedstock can also facilitate the ink flow if the viscosity of the materials is temperature dependent. The printing parameters must be optimized for each feedstock material in SSE and it is necessary to keep the printing parameters under control to avoid weight variability during the printing process (Díaz-Torres et al., 2021). The optimization of printing parameters can be time consuming, so new tools to characterize the potential ink and to understand the complexity of the feed-stock materials are required (Díaz-Torres et al., 2021; Zidan et al., 2018a; Zidan et al., 2018b).

Quality by test (QbT) is the conventional strategy described in pharmacopoeias to ensure the quality and subsequent release of a batch (Zhang and Mao, 2017). These tests are generally destructive and require a considerable number of dosage units (Yu et al., 2014; Zhang



Fig. 2. Diagram of compression/shrinkage cycle, showing the two extrusion speeds tested: A) 0.05 mm/s and B) 0.15 mm/s.

and Mao, 2017), making this approach incompatible with on-demand fabrication of personalized medicines using 3D printing. In particular, the required sample size for quality control by QbT can be more than the actual number of dosage units required by the patient. Also, QbT of the intermediate product, namely the mass to be extruded, is commonly carried out using expensive rheometry or texture analysis that can hardly emulate all the stress conditions that the masses are subjected to during the 3D printing process, leaving some variables uncontrolled.

As such, the implementation of quality by design (QbD) approaches has seen considerable interest in the production of personalized medicines using 3D printing (Crişan et al., 2022; Rahman et al., 2021; Zhang et al., 2020). Foremost, it is important to identify critical process parameters (CPP) and CQA of the final dosage form. Thus far, these printed dosage forms lack any regulatory specifications (Rahman and Quodbach, 2021); nonetheless, discussions are being held in various countries, such as the United Kingdom, on new regulations to facilitate the implementation of 3D printing at the point-of-care (MHRA, 2022). The use of process analytical technology (PAT) may allow the manufacturing process to be controlled in a multivariate statistically significant way (MSPC) by means of non-destructive analytical techniques, allowing the correction of errors detected in-line or the elimination of dosage forms that do not meet the established quality criteria from each batch (Europe, 2021a, 2021b). Real-time batch release of 3D printed dosage forms is necessary, and appropriate control strategies and PATs are

needed to monitor the CQAs. The implementation of PAT in the control systems is also essential to optimize the quality of the finished dosage form (Rahman and Quodbach, 2021). Researchers have identified some CPPs for 3D printing of medicines such as printing surfaces, first layer height (FLH), fill density, filament diameter, and nozzle diameter (Díaz-Torres et al., 2021; Zidan et al., 2018a; Zidan et al., 2018b). Rheological behaviour of the ink is also a critical attribute that requires fine tuning of relevant CPP, such as nozzle diameter and printing rate. Therefore, there is an urgent unmet need for the development of in-line control protocols for SSE 3D printing.

The aim of this study is to implement, for the first time, a pressure sensor in an SSE pharmaceutical 3D printer to obtain useful information regarding material properties and as a PAT. This pressure sensor may first endow the pharmaceutical 3D printer with in situ texturometer capabilities for the characterization of the materials. This tool would allow the control of the process parameters during both the testing of the inks under printing-like conditions and then the printing process of the medicines. Three different masses, vaseline (as high flow material model), gel-like formulation (isoleucine chewable gel-based formulation as temperature-stimuli response material), and paste-like formulation (isoleucine formulation paste based as extrudable material at room temperature) were evaluated. Different flow parameters were recorded for the characterization of the masses, and relationship between the flow properties and the printability were attempted. The outcomes obtained

Step 1

Enter the basic properties of the test

✓

Project name

Syringe inner diameter
 mm.

Activation force
 N On Off

Heater_sleep
 °C On Off

Sample name

Nozzle inner diameter

Starting temperature
 °C On Off

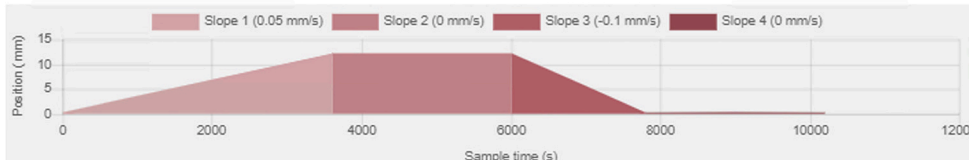
Step 2

Set up the programme for the test you wish to perform

⌚

Distance mode (mm) Volume mode (mm³)

Slope 1 (0.05 mm/s) Slope 2 (0 mm/s) Slope 3 (-0.1 mm/s) Slope 4 (0 mm/s)



	Speed (mm/s)	Distance (mm)	Time (seconds)	Temperature (°C)	
1	<input type="text" value="0,05"/>	<input type="text" value="3"/>	<input type="text" value="60,00"/>	<input type="text" value="37"/>	✕
2	<input type="text" value="0,00"/>	<input type="text" value="0,00"/>	<input type="text" value="40,00"/>	<input type="text" value="37"/>	✕
3	<input type="text" value="-0,10"/>	<input type="text" value="3"/>	<input type="text" value="30,00"/>	<input type="text" value="37"/>	✕
4	<input type="text" value="0,00"/>	<input type="text" value="0,00"/>	<input type="text" value="40"/>	<input type="text" value="37"/>	✕

Fig. 3. Screenshot of the Texturometer Utility for M3DIMAKER Studio (FabRx Ltd., UK), showing the program created for the compression/shrinkage cycle, with test conditions and data collection.

with the new sensors were compared and validated using a conventional rheometer.

2. Materials and methods

2.1. Materials

Chewable gel-based formulation was provided by FabRx Ltd. (United Kingdom). L-Isoleucine was purchased from Nutricia (Netherlands). Vaseline soft, polyvinylpyrrolidone (PVP) and oral banana essence were provided by Acofarma. Ac-Di-Sol® (Croscarmellose Sodium) was provided by FMC Corporation (Philadelphia, PA, USA). Lactose monohydrate was purchased from Sigma-Aldrich (St. Louis, MO, USA).

2.2. Preparation of extruded masses

Three masses with different expected rheological and flow

characteristics were selected and tested.

2.2.1. Vaseline soft

Commercial vaseline soft or white soft paraffin was chosen as a model compound since its flow and rheological properties have been extensively studied (Barry and Grace, 1971). According to previous reports, it has a temperature dependent behaviour which makes it suitable for our test conditions.

2.2.2. Gel-like formulation

Chewable gel-based formulation containing 40% w/w of isoleucine was prepared as temperature-responsive material. The composition of the chewable formulation from FabRx includes sucrose, pectin, maltodextrin, maltitol, buffer salts and water. All the excipients were added to a metal container and mixed with a blade stirrer (Heidolph, Germany). The mixture was heated to 80 °C for 10 min on a hot plate with temperature control (MS-H280-Pro model) and isoleucine was added until

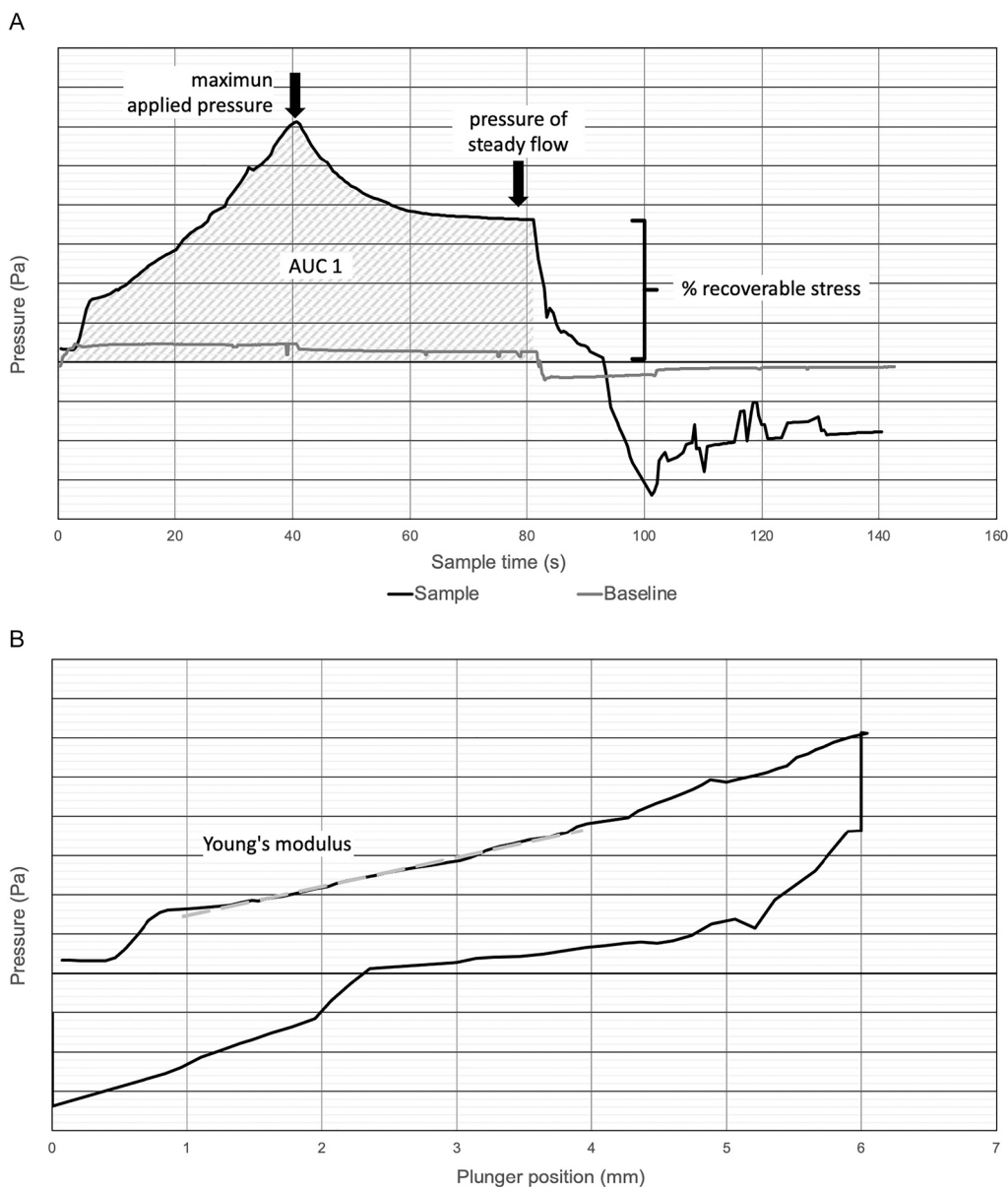


Fig. 4. Example of graphical representation for test profile B of (A) the pressure applied versus test time (graphical calculation of the flow parameters for each mass) and (B) of the pressure exerted versus the displacement of the piston (graphical calculation of the Young's modulus for each mass).

Table 2 Studied parameters.

Name	Units	Data source	Calculation
Maximum applied pressure (MAP)	Pa	Laguna SSE printhead	Pressure-time plot
Pressure of steady flow (PSF)	Pa	Laguna SSE printhead	Pressure-time plot
Recoverable stress	%	Laguna SSE printhead	Pressure-time plot (PSF / MAP) * 100
Time to reach steady flow	S	Laguna SSE printhead	
Yield stress	Pa	Laguna SSE printhead	Pressure-time plot
Young module	Pa	Laguna SSE printhead	Pressure-displacement plot
Dynamic viscosity (μ)	Pa·s	Rheometer	$\mu = \frac{\tau}{\dot{\gamma}}$
Shear stress (τ)	Pa	Rheometer	
Storage modulus (G')	Pa	Rheometer	
Loss modulus (G'')	Pa	Rheometer	

completely dispersed in the mass. Finally, the syringes were filled with the formulation and cooled to room temperature for pectin gelation.

2.2.3. Paste-like formulation

For the preparation of the paste containing isoleucine (40.4% w/w), all the components were milled separately using a mortar and pestle. Each component was then added to the Unguator® mixer jar in the following order: isoleucine, lactose monohydrate (18.2% w/w), polyvinyl pyrrolidone 30 K (8.1% w/w), banana flavouring essence (3.0% w/w), and Ac-Di-Sol (30.3% w/w). Purified water was gradually added, mixing for 20 s at 600 rpm at each interval, until a 40:60 solid:water mass ratio was obtained.

2.3. Texture analysis using a 3D printer pressure instrumentalized SSE printhead

A pharmaceutical 3D printing platform (M3DIMAKER, FabRx Ltd., UK) equipped with the pressure instrumentalized SSE motor-driven printhead (Laguna SSE printhead, FabRx Ltd., UK) was used (Fig. 1).

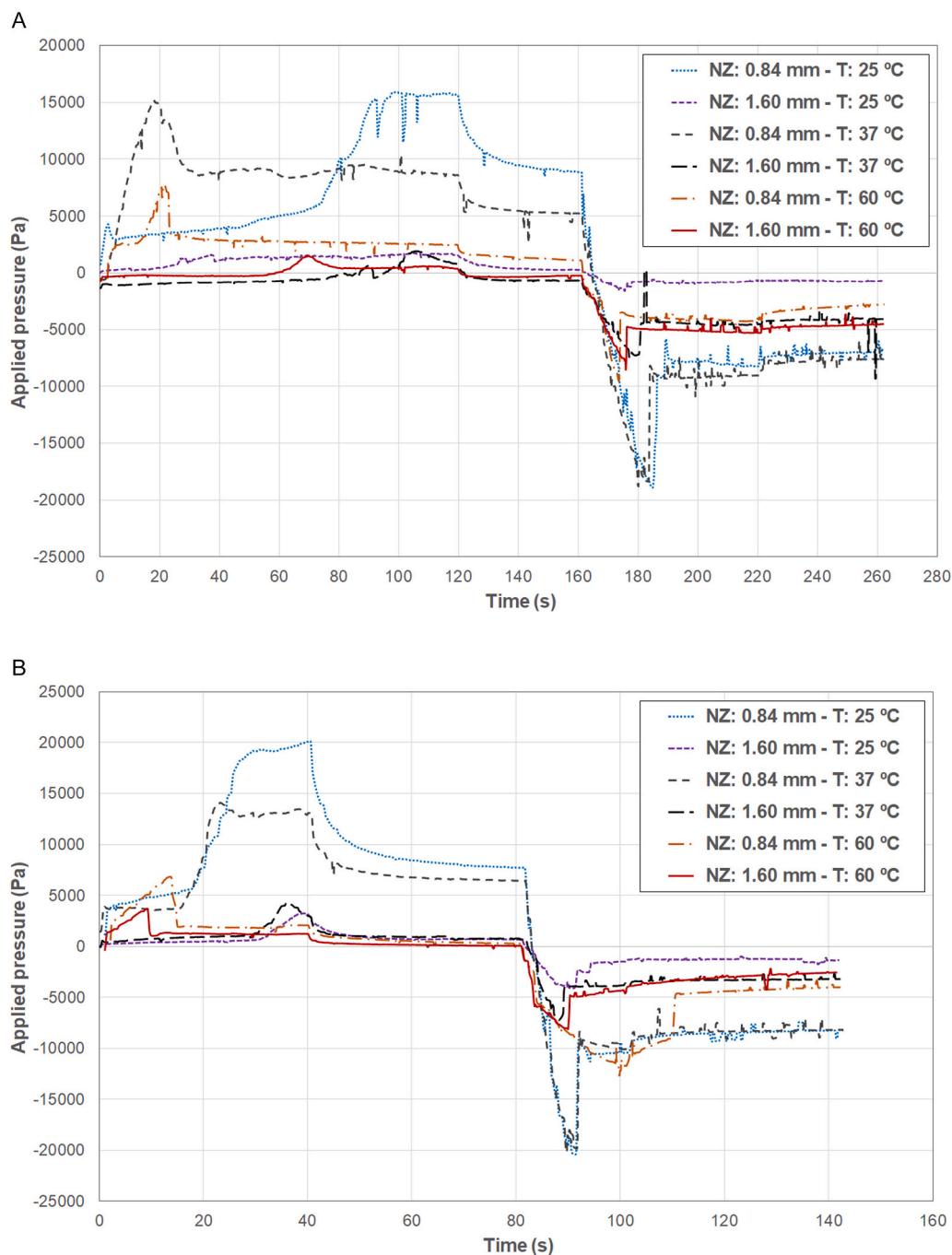


Fig. 5. Graphical representation of the applied pressure versus time recorded for commercial soft vaseline using A) the test profile A ($Q = 16.02 \text{ mm}^3/\text{s}$) and B) test profile B ($Q = 48.07 \text{ mm}^3/\text{s}$). Two nozzle sizes (NZ), (0.84 and 1.60 mm) and three temperatures (T) (25 °C, 37 °C, 60 °C) were evaluated.

In contrast to other 3DP SSE technologies, this brand-new printhead performs mechanical extrusion by using an anchoring system with a stepper motor. In this way, the syringe plunger could move with millimetric precision to achieve precise dosing of the semi-solid mass. This printhead is designed to fit a 20 mL syringe (B. Braun Medical Inc. OEM, UK) in which the materials to be extruded are introduced. Approximately 15 g of each of the prepared masses were loaded through the back of the syringes using a spatula.

The extrudability profile describes the force applied as a function of time, required to extrude a formulation at a specified flow rate through a nozzle of defined length and tip diameter and at a given temperature. Two conical extrusion nozzles (1.60 mm or 0.84 mm orifices), two flow values and three extrusion temperatures were studied (Table 1).

Using the Texturometer Utility for M3DIMAKER Studio (FabRx Ltd., UK) integrated in the pharmaceutical 3D printing platform, it was possible to set up the compression/shrinkage cycle. The compression/shrinkage cycle (Fig. 2) consisted of applying a downward force on the plunger cartridge for a distance of 6 mm, followed by a hold time of 40 s, then a retraction of the same distance previously travelled, and finally a waiting time of 40 s.

In this way, two compression/shrinkage profiles were used to perform the different tests in which the plunger displacement speed was varied (0.05 mm/s (Profile A) and 0.15 mm/s (Profile B)) in order to simulate the semi-solid material flows that are used during 3D printing at low printing speed and at high printing speed, respectively, through the different nozzle gauges used.

Table 3

Results of soft vaseline characterization using the instrumented plunger of the Laguna SSE printhead.

Formulation	Temp. (°C)	Q (mm ³ /s)	Nozzle inner diameter (mm)	Maximum applied pressure (Pa · 10 ⁵)	Steady flow pressure (Pa · 10 ⁵)	Recoverable stress (%)	AUC 1 (Pa · s · 10 ⁶)	Young's modulus (Pa · 10 ⁴)
Soft vaseline	25	48.07	0.84	0.201	0.080	39.85	0.818	0.062
Soft vaseline	25	48.07	1.60	0.033	0.007	21.92	0.072	0.220
Soft vaseline	25	16.02	0.84	0.159	0.100	62.83	1.320	0.851
Soft vaseline	25	16.02	1.60	0.018	0.005	27.95	0.163	0.064
Soft vaseline	37	48.07	0.84	0.141	0.066	46.62	0.640	0.992
Soft vaseline	37	48.07	1.60	0.043	0.009	19.72	0.098	0.296
Soft vaseline	37	16.02	0.84	0.151	0.056	36.85	1.299	1.864
Soft vaseline	37	16.02	1.60	0.018	0.005	27.95	0.163	0.056
Soft vaseline	60	48.07	0.84	0.069	0.004	5.71	0.132	n.d.
Soft vaseline	60	48.07	1.60	0.037	0.001	2.39	0.064	n.d.
Soft vaseline	60	16.02	0.84	0.077	0.014	18.05	0.399	n.d.
Soft vaseline	60	16.02	1.60	0.015	-0.003	-19.47	0.007	n.d.

For each of the pharmaceutical formulations selected in this study, 12 trials were carried out to evaluate the effects of three variables of the 3D printing process (nozzle inner diameter, flow or extrusion speed and extrusion temperature) on the rheological properties of the semi-solid masses (Table 1). The levels of each of the variables studied were selected to mimic different printing conditions.

For each parameters combination, compression/shrinkage cycles were performed with the syringe empty to record a baseline that may correct the signal derived exclusively from the friction of the instrumented plunger against the syringe walls.

Data collection and subsequent analysis were done using the Texturometer Utility for M3DIMAKER Studio (FabRx Ltd., UK) (Fig. 3).

Based on the resultant pressure-time plot, some extrudability parameters such as maximum applied pressure, pressure of steady flow, and recoverable stress percentage were determined (Fig. 4A) for each formulation and set of parameters.

From the plots of pressure versus displacement (Fig. 4B), some parameters of interest to characterize the rheological behaviour of the masses were obtained, such as the Young's modulus and the area under the curve to calculate the work required to perform the extrusion (Table 2).

2.4. Rheological characterization

Each syringe mass was sampled and mechanically analysed with a rheometer (Anton Paar, MCR 302, Austria) equipped with a Peltier HPTD 200 hood and a disposable aluminium measuring plate (15 mm diameter). G' (storage modulus) and G'' (loss modulus) were recorded during a self-healing test (amplitude sweep mode at 1 Hz) consisting in five steps in which the shear strain was alternatively changed from 0.5% (300 s) to 100.0% (120 s) to mimic the mass at rest conditions and the mass extruded at high rate through the nozzle, respectively (Conceicao et al., 2019). The gap and the temperature were set at 1 mm and 20 °C, respectively.

2.5. 3D printing

A 3D model file was generated (.stl file) containing a total of 30 cylinders (8.20 mm diameter × 4.10 mm height), each separated by 1 cm using Autodesk® Fusion 360 (version 2.0.9011, Autodesk Inc., California, USA). The 3D models were sliced directly using the software Slic3r (version 1.3.1-dev, GNU Affero General Public License) open-source 3D printing toolbox integrated in Repetier Host software (version 2.1.6, Hot-World GmbH & Co. KG, Willich, Germany). The obtained gcode files were sent to the printer using Repetier Host software.

The built-in data logger of the M3DIMAKER 3D printing platform was used to collect the applied pressure values of the Laguna SSE printhead to check that the process remained under control during the entire production of the printlets, and to detect possible obstructions or

the presence of air that could affect the final quality attributes (CQA) of the dosage forms. 3D scatter representation of the pressure values during the production of the batch of dosage forms for each coordinate in space (X, Y, Z) were plotted.

3. Results and discussion

In the present study, a pressure sensor was connected to the extrusion barrel of the 3D printer for real-time recording of flow properties of semi-solid masses through the small-gauge nozzles used in the production of printlets. The use of the syringe employed during printing as well as the use of the 3D printing platform itself eliminates many variables that must be controlled if the tests were performed in the traditional way; namely, using a rheometer, texturometer or other equipment for testing the ink candidates before printing. In a simpler way, the developed setup permitted short experiments to be conducted using the printing platform itself. Not only does this emulate the exact printing conditions, 3D printing may also be commenced immediately using the identified optimal parameter values.

The pressure instrumented SSE motor-driven printhead (Laguna SSE printhead, FabRx Ltd., UK) and its control software allowed the characterization of the mass under the same conditions as that during printing. It was possible to emulate the movements made by the plunger over the mass during the printing process with the same heating chamber, syringe and nozzle, thus being able to determine the mechanical properties of the mass in situ. This eliminates numerous other confounding factors, such as heat diffusion or flow through the nozzle and syringe barrel walls.

3.1. Texture analysis

For the texture analysis model, the applied pressure shown in Fig. 4 was the actuation pressure applied by the plunger of the printhead. The compression/shrinkage cycles showed a common pattern, with a gradual increase in pressure until a threshold was reached where the mass began to flow through the nozzle. A steady flow was then achieved under a constant applied driving force. Subsequently, after the applied force was released, the pressure decreased at different rates depending on the type of mass studied, until reaching a plateau that coincided with the moment when the mass stopped flowing throughout the nozzle.

By carrying out the different experiments, it was possible to estimate the percentage of recoverable stress and to determine which type of behaviour predominates in each of the masses (plastic behaviour, viscoelastic behaviour, elastic behaviour). An important difference was found between the gel-like formulation and the paste-like formulation after cessation of extrusion force, as described below. The yield stress pressure required to initiate the flow was estimated from the plot of the pressure applied versus time.

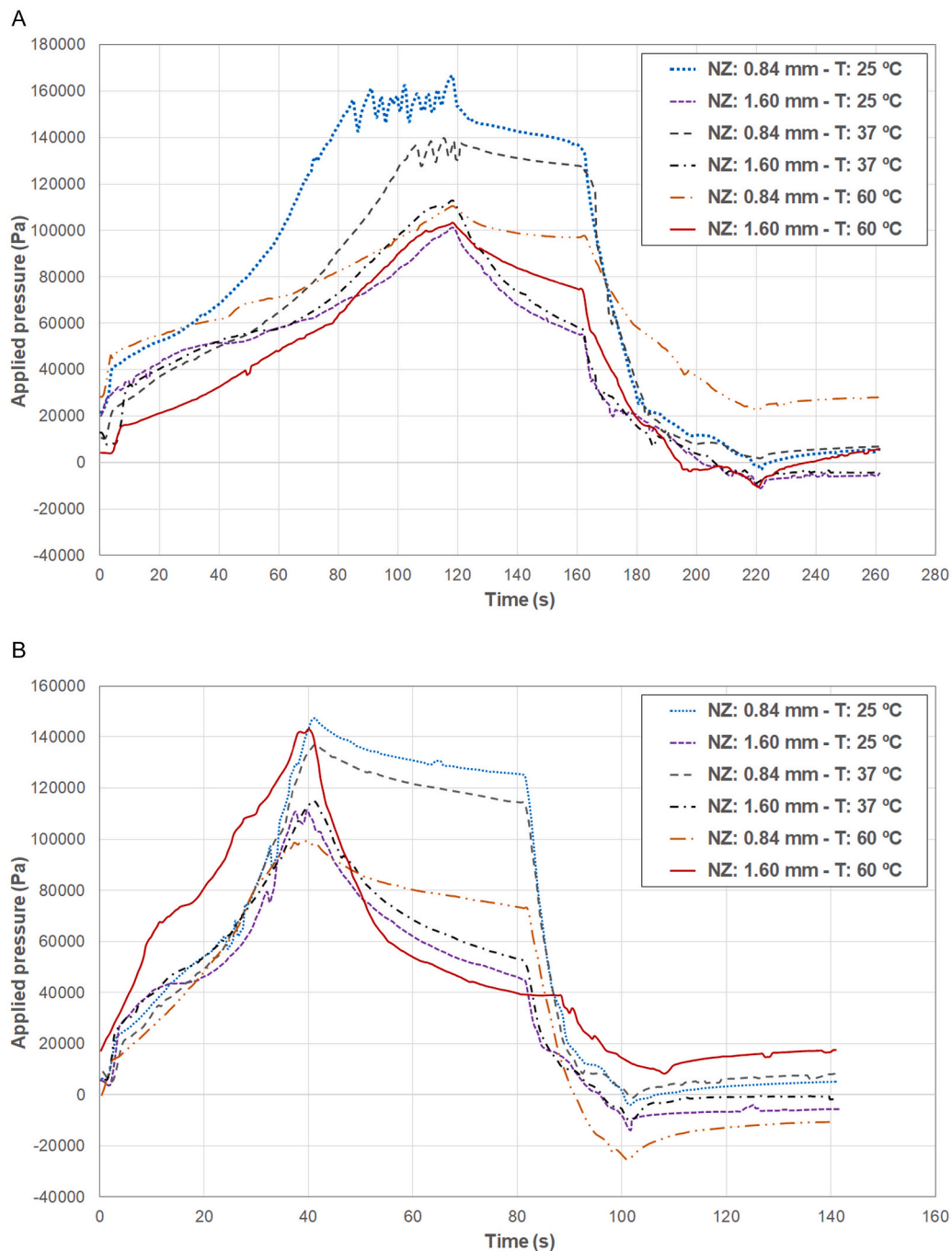


Fig. 6. Graphical representation of the applied pressure versus time for the gel-like formulation using A) the test profile A ($Q = 16.02 \text{ mm}^3/\text{s}$) and B) test profile B ($Q = 48.07 \text{ mm}^3/\text{s}$). Two nozzle sizes (NZ), (0.84 and 1.60 mm) and three temperatures (T) (25 °C, 37 °C, 60 °C) were evaluated.

3.1.1.1. Soft Vaseline

Soft vaseline or white soft paraffin presented a temperature-dependent behaviour as shown in Fig. 5 and Table 3. When the compression/shrinkage cycle profile A (Fig. 5A) with lower flow rate ($16.02 \text{ mm}^3/\text{s}$) was used, some differences were found between experiments carried out with the lower diameter nozzle (0.84 mm), depending on the temperature set for the test. When the temperature was set at 25 °C the maximum pressure applied was higher than for the test carried out at 37 °C. As expected, in the case of the test carried out at 60 °C with this nozzle, the value of the maximum applied pressure was even lower (Barry and Grace, 1971). In this way, the viscosity of the soft vaseline decreased with increasing temperature.

The application of profile B performed at higher flow rate (48.07

mm^3/s) evidenced that the maximum pressure was obtained with the use of the lowest temperature (25 °C) and with the smallest nozzle diameter (0.84 mm). In the test performed at 37 °C using this nozzle, a decrease in the maximum pressure occurred due to the decrease in viscosity and greater ease of flow. In the experiments carried out with the larger diameter nozzle (1.60 mm), no significant differences were observed between the extrusions carried out at 25 °C and at 37 °C. For the tests carried out at 60 °C using both nozzles, the mass showed a notably different behaviour, in line with previous publications (Barry and Grace, 1971).

The percentage of recoverable stress was relatively low (19.72% - 62.83%) for all test conditions at 25 °C and 37 °C, particularly when the larger internal diameter nozzle (1.60 mm) was used. With this nozzle

Table 4

Results of gel-like formulation characterization using the instrumented plunger of the Laguna SSE printhead.

Formulation	Temp. (°C)	Q (mm ³ /s)	Nozzle inner diameter (mm)	Maximum applied pressure (Pa · 10 ⁵)	Steady flow pressure (Pa · 10 ⁵)	Recoverable stress (%)	AUC 1 (Pa · s · 10 ⁶)	Young's modulus (Pa · 10 ⁴)
Gel-like formulation	25	48.07	0.84	1.472	0.053	3.59	7.819	1.345
Gel-like formulation	25	48.07	1.60	1.113	0.545	48.99	4.890	1.444
Gel-like formulation	25	16.02	0.84	1.667	1.432	85.92	18.369	1.674
Gel-like formulation	25	16.02	1.60	1.012	0.654	64.59	10.206	0.934
Gel-like formulation	37	48.07	0.84	1.369	1.180	86.16	7.370	1.258
Gel-like formulation	37	48.07	1.60	1.152	0.641	55.66	5.349	1.022
Gel-like formulation	37	16.02	0.84	1.397	1.315	94.09	14.237	1.303
Gel-like formulation	37	16.02	1.60	1.128	0.701	62.21	10.826	1.256
Gel-like formulation	60	48.07	0.84	1.590	1.375	86.47	10.253	1.387
Gel-like formulation	60	48.07	1.60	1.430	0.417	29.17	6.181	1.684
Gel-like formulation	60	16.02	0.84	1.106	0.985	89.05	12.970	0.743
Gel-like formulation	60	16.02	1.60	1.032	0.828	80.24	9.657	1.133

(1.60 mm), it is likely that vaseline continued flowing to some extent after the plunger displacement has stopped, and this mass displacement may have made the pressure drop more sharply. In the case of the tests carried out at 60 °C, the percentage of recoverable stress was <5% under all conditions, in good agreement with the drop in viscosity exhibited by vaseline when heated.

Young's modulus was determined from the initial slope of the resulting stress-strain curves. The soft vaseline showed temperature-independent but flow rate-dependent Young's modulus values for the experiments carried out with the largest internal diameter nozzle (1.60 mm). A lower value was recorded when profile A was applied (16.02 mm³/s), compared to when profile B was applied (48.07 mm³/s), with the values being ≈ 2.5 kPa and ≈ 0.6 kPa respectively. Due to the incongruent behaviour of soft vaseline at 60 °C, the Young's modulus values of these experiments could not be determined.

3.1.2. Gel-like formulation for chewable printlet

The formulation designed to produce chewable dosage forms showed temperature-sensitive behaviour (Fig. 6 and Table 4). The tests carried out following the cycle profile A and lower mass flow (16.02 mm³/s) (Fig. 6A) revealed that the maximum applied pressure was higher for the tests carried out at 37 °C than for those carried out at 60 °C. Using the smallest nozzle diameter (0.84 mm) and 37 °C, the highest applied pressure, $1.39 \cdot 10^5$ Pa, was required. The applied pressure value for the other nozzle-temperature variable pairs was around $1.10 \cdot 10^5$ Pa.

The recoverable stress recorded at 37 °C and 60 °C using the smaller diameter nozzle (0.84 mm) was $\geq 89.05\%$. When the larger diameter nozzle (1.60 mm) was used at 37 °C, there was a significant drop in pressure within a few seconds, reaching the steady state pressure quickly and showing a recoverable stress rate of <65%.

As shown in Fig. 6B, when the cycle profile B and the highest flow (48.07 mm³/s) were applied, the highest applied pressure values were recorded when the smallest nozzle diameter (0.84 mm) was used. The values increased when lower extrusion temperatures were set, for example, at 25 °C and smaller inner diameter nozzle (0.84 mm) the maximum applied pressure ($\approx 1.5 \cdot 10^5$ Pa) was reached.

The experiments carried out at 60 °C at this flow rate showed important differences depending on the nozzle used. When the smaller diameter nozzle (0.84 mm) was used, high values of pressure in the

steady flow and percentage of recoverable stress were obtained. Under these conditions, it took more time both to reach the required flow and to stop the flow. Thus, the control of the semi-solid mass dosing on the printing surface was worse. Differently, the behaviour observed for the larger diameter nozzle (1.60 mm) was more suitable since within a short period of time (< 5 s), there was a significant decrease in pressure and the flow stopped, which in turn led to more precise control of the dosage of the 3D printing ink. The recoverable stress for this set of parameters (60 °C, 1.60 mm) was considerably lower (29.17%) than for the remaining experimental conditions (> 55%). According to the obtained results, the most suitable set of printing parameters for the gel-like formulation is a temperature of 60 °C, a nozzle of a large diameter (e. g. 1.60 mm (14 gauge)), and a high printing speed. The flow rate of 48.07 mm³/s is equivalent to high printing speeds such as 20 mm/s when a 3DP layer height equal to the internal diameter of the nozzle is set. A similar formulation with different isoleucine content was successfully 3D printed and tested in a clinical study (Goyanes et al., 2019).

Young's modulus was determined from the initial slope of the resulting stress-strain curves. The gel-like mass showed similar Young's modulus values (≈ 10 kPa), regardless of the nozzle, extrusion speed or temperature employed (Table 4).

3.1.3. Paste-like formulation

The formulation designed to produce orodispersible printlets based on cellulose derivatives was less sensitive to temperature changes in the range evaluated (Fig. 7 and Table 5).

Applying cycle A and low flow rate (16.02 mm³/s), the maximum pressure was $1.77 \cdot 10^5$ Pa for the smallest diameter nozzle (0.84 mm) and for the lowest test temperature (25 °C) (Fig. 7A). When the nozzle used was the smaller diameter (0.84 mm), the maximum extrusion pressure and stationary flow pressure values were much higher at 37 °C than at 60 °C for the same flow rate. The recoverable stress percentage was dependent on the nozzle used, being lower for the larger diameter nozzle (1.60 mm), with no important differences being observed as a function of temperature for this nozzle, being almost the same for the experiments carried out at 25 °C and 37 °C ($\approx 67\%$) and slightly lower for the experiment carried out at 60 °C ($\approx 55\%$). A discernible difference was measured in the test carried out at 37 °C versus 20 °C and 60 °C with the smaller diameter nozzle (0.84 mm) and lower flow rate (16.02 mm³/

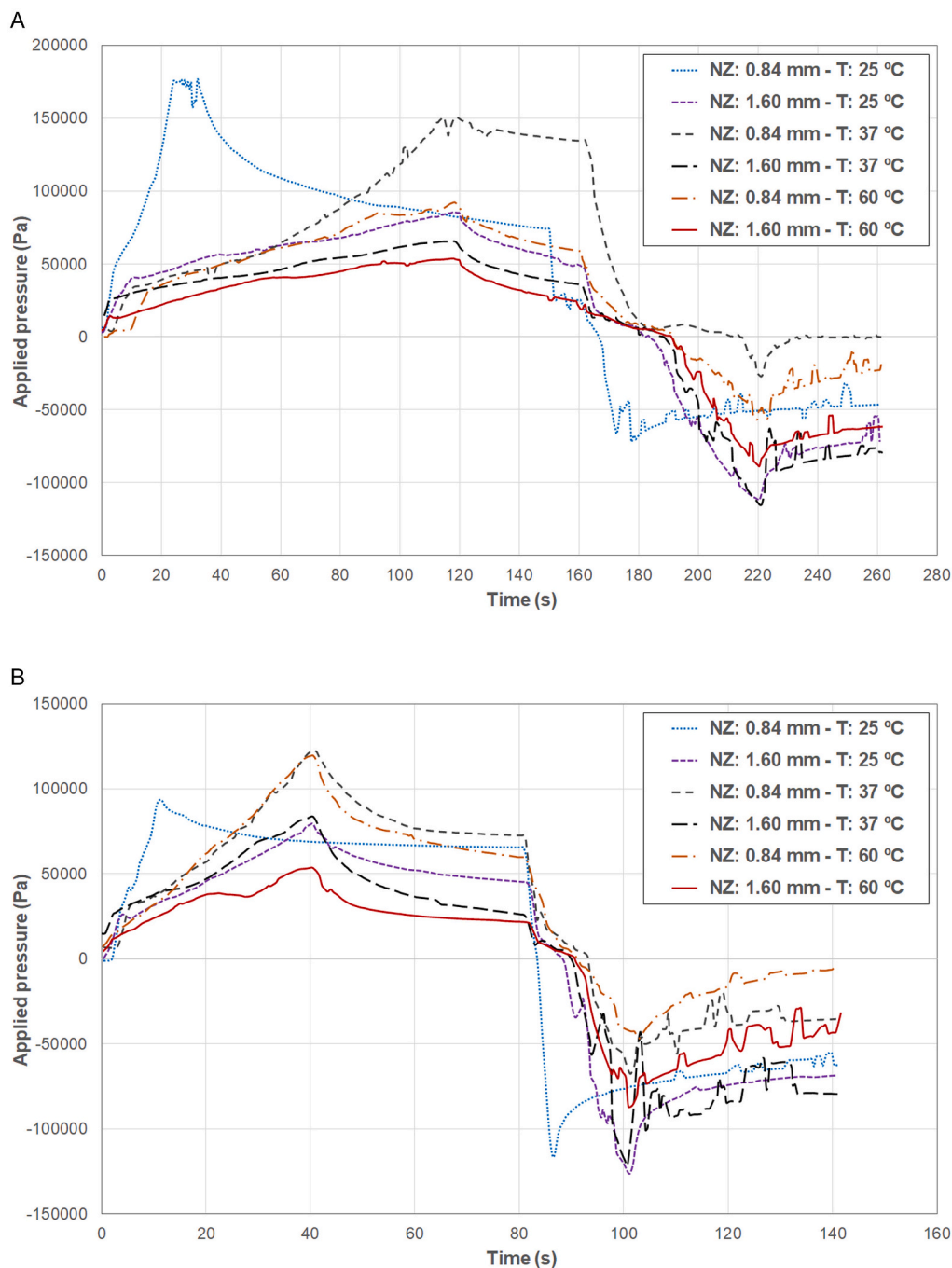


Fig. 7. Graphical representation of the applied pressure versus time for the paste-like formulation sample using (A) the test profile A ($Q = 16.02 \text{ mm}^3/\text{s}$) and (B) test profile B ($Q = 48.07 \text{ mm}^3/\text{s}$). Two nozzle sizes (NZ), (0.84 and 1.60 mm) and three temperatures (T) (25 °C, 37 °C, 60 °C) were evaluated.

s), where the recoverable stress percentage was considerably higher (> 90%) as the stationary flow pressure ($\approx 1.40 \cdot 10^5 \text{ Pa}$).

Considering the pressure at steady flow recorded, for the highest flow rate ($48.07 \text{ mm}^3/\text{s}$), the mass flow through the nozzle ceases at around $7.00 \cdot 10^4 \text{ Pa}$ for the lower diameter nozzle (0.84 mm) and $3.00 \cdot 10^4 \text{ Pa}$ for the larger diameter nozzle (1.60 mm) regardless of the temperature used (37 °C or 60 °C). In the tests carried out using the cycle profile B and the highest flowrate ($48.07 \text{ mm}^3/\text{s}$), the pressure at steady flow as well as the maximum pressure depended mainly on the nozzle size used. As expected, the highest-pressure values were recorded for the lower nozzle diameter (0.84 mm).

In all cases presented in Fig. 7B, the pressure value dropped quickly in <10 s, and the recoverable stress percentages were lower, ranging

from 36.76% (1.60 mm nozzle) to 60.43% (0.84 mm nozzle) at 37 °C.

The paste-like mass showed similar Young's modulus values ($\approx 10 \text{ kPa}$) for measurements performed at 37 °C and 60 °C, regardless of the nozzle used or extrusion speed. The highest values of Young's modulus for these temperatures were recorded when the smallest diameter nozzle (0.84 mm) and the highest flowrate ($48.07 \text{ mm}^3/\text{s}$) were used ($\approx 18 \text{ kPa}$).

Based on the results obtained, there are several sets of parameters that are postulated as adequate for appropriate flow properties of the isoleucine-loaded paste-like formulation to produce printlets with desirable quality attributes. Using a high flow rate $48.07 \text{ mm}^3/\text{s}$ (high printing speed), these parameters are a printing temperature between 37 °C - 60 °C and a nozzle diameter (1.60 mm or even 0.84 mm)

Table 5

Results of paste-like formulation characterization using the instrumentised plunger of the Laguna SSE printhead.

Formulation	Temp. (°C)	Q (mm ³ /s)	Nozzle inner diameter (mm)	Maximum applied pressure (Pa · 10 ⁵)	Steady flow pressure (Pa · 10 ⁵)	Recoverable stress (%)	AUC1 (Pa·s · 10 ⁶)	Young's modulus (Pa · 10 ⁴)
Paste-like formulation	25	48.07	0.84	0.935	0.671	71.78	5.376	5.690
Paste-like formulation	25	48.07	1.60	0.792	0.482	60.83	4.027	0.988
Paste-like formulation	25	16.02	0.84	1.766	0.841	47.61	15.244	10.723
Paste-like formulation	25	16.02	1.60	0.856	0.576	67.22	9.729	0.738
Paste-like formulation	37	48.07	0.84	1.225	0.740	60.43	5.878	1.833
Paste-like formulation	37	48.07	1.60	0.836	0.307	36.76	3.720	1.422
Paste-like formulation	37	16.02	0.84	1.511	1.397	92.41	14.559	1.029
Paste-like formulation	37	16.02	1.60	0.657	0.445	67.70	7.454	0.686
Paste-like formulation	60	48.07	0.84	1.194	0.666	55.78	5.522	1.896
Paste-like formulation	60	48.07	1.60	0.536	0.246	45.91	2.470	0.975
Paste-like formulation	60	16.02	0.84	0.924	0.654	70.83	9.743	1.223
Paste-like formulation	60	16.02	1.60	0.540	0.301	55.68	5.870	1.129

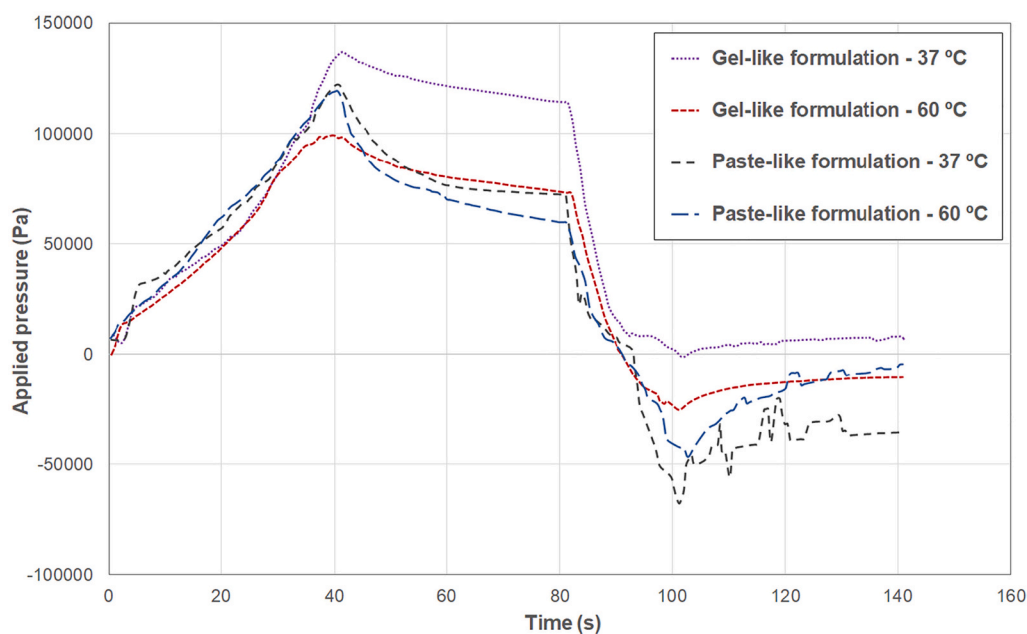


Fig. 8. Graphical representation of the applied pressure versus time for the gel-like and paste-like formulation sample using test profile B ($Q = 48.07 \text{ mm}^3/\text{s}$) smaller nozzle diameter (NZ), (0.84 mm) and two temperatures (T) (37 °C, 60 °C) were compared.

depending on the resolution of the 3D object to be created. A similar composition has already been previously 3D printed containing hydrochlorothiazide as the active pharmaceutical ingredient (Díaz-Torres et al., 2021).

3.1.4. Gel-like vs paste-like formulation

As inferred from the pressure versus time plots recorded in the 3D printer, the rheological properties of the gel-like mass and the paste-like mass, both containing isoleucine, were different (Fig. 8). The mass containing AcDiSol (paste-like) presented a lower percentage and higher rate of recoverable stress after stopping extrusion at 40 s, regardless of the temperature used, reaching the steady flow pressure after 20 s,

which indicates a mostly viscoelastic behaviour. On the other hand, the gel-like mass presented a considerably slower recoverable stress than the paste-like mass and in a much higher percentage, which indicated a more plastic behaviour. Based on the differences observed in the maximum applied pressure and in the steady flow pressure for this mass at the different temperatures, it can be concluded that it shows a temperature-dependent behaviour.

3.2. Rheological characterization

The prepared masses were tested in parallel in a rheometer in order to validate the information on viscoelasticity inferred from the 3D

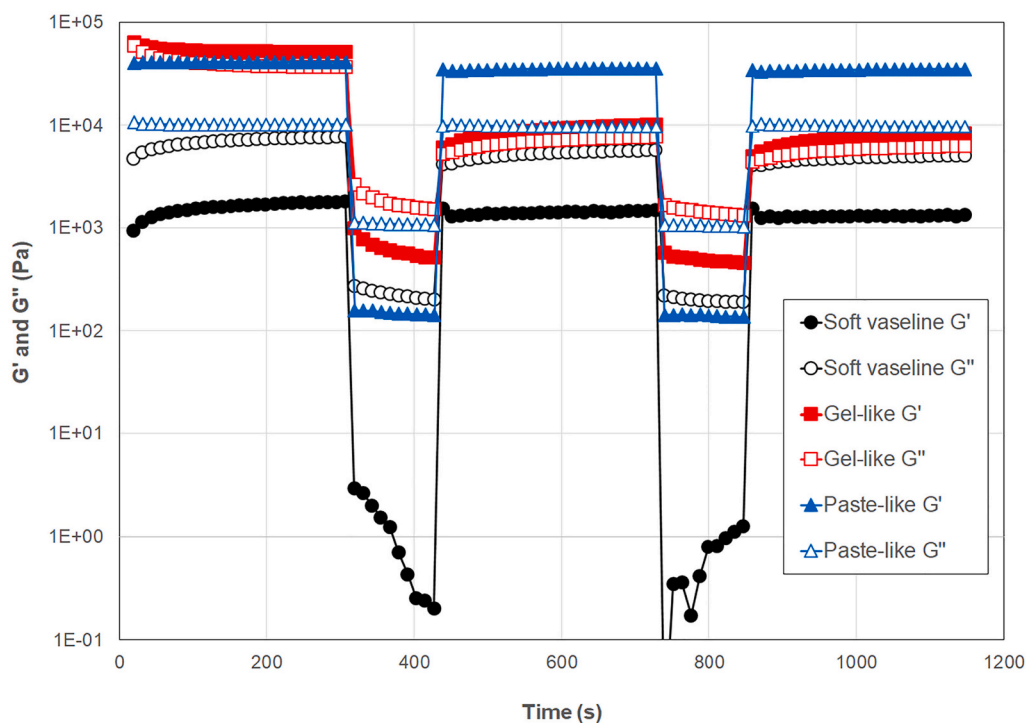


Fig. 9. Rheological properties of the masses.

printer plots. The semi-solid masses were loaded into the printer syringe and a portion was poured on the plate of the rheometer to study the dependence of G' and G'' on applied strain.

Amplitude sweep tests were recorded under strain conditions that mimic rest-like situation in the syringe barrel (0.5% strain) and then maximum stress (100% strain) during extrusion through the nozzle. These conditions were applied cyclically to obtain information on the consistency of recovery once the wet mass was deposited on the 3D printing surface and the feasibility of using the same mass for successive printing of several printlets. The protocol chosen was similar to that previously proposed for evaluating self-healing materials (Borre et al., 2015) and stimuli-responsive gels for 3D printing (Zhang et al., 2015).

The range of applied strain (from 0.5 to 100%) was the same as that previously evaluated by other authors for related wet masses (Conceicao et al., 2019) in order to cover the most extreme situations that the semisolid masses can face during 3D printing (Fig. 9).

Among the three tested formulations, vaseline had the lowest G' values under all strain conditions tested, with a clear predominance of the viscous component. G'' was one order of magnitude greater than G' . This means that under an applied stress, vaseline deforms and flows with minor storage of energy. In terms of 3D printing this means that, compared to the other tested formulations, vaseline requires less pressure to start to flow and that the diameter of the strut will be similar to that of the nozzle with minor increase in width. Also, in this regard, after the strong strain suffered during the pass through the nozzle, G' and G'' values rapidly recovered and reached the same values as in the rest before printing, which ensures good fidelity to the design. In good agreement with the viscoelastic behaviour recorded in the rheometer, the pressure instrumentalized plunger coupled to the 3D printer demonstrated low pressure required to achieve the desired flow and low percentage of pressure recovered.

While both the gel-like and paste-like formulations had G' values larger than G'' values at rest, the paste-like formulation showed a clear predominance of the G' values, i.e. a more solid-like behaviour. The gel-like formulation underwent an abrupt decrease in G' from 51 KPa to 0.6 KPa when the strain was maximum, and then recovered to 10 KPa in 2 min at rest. In the case of G'' , the values rapidly decreased from 36 KPa to

1.5 KPa at maximum strain and then increased to 7 KPa in 2 min at rest. This behaviour indicates that although the gel-like formulation has self-healing capability, the recovery at rest is not immediate, suggesting shear-thinning and thixotropic behaviour. The large values of G' explain the large recovery of energy when the plunger stops the movement downward, particularly under the most stressful conditions of the delivery through the smallest diameter nozzle. The incomplete recovery of the moduli in a short time also explains that the stress needed for retraction was low.

In the case of paste-like formulation, the loss modulus was smaller with values of 10 KPa at rest, compared to G' which was 40 KPa. Remarkably, the paste-like formulation exhibited very rapid loss of both moduli under 100% strain (G' : 0.15 KPa; G'' : 1.0 KPa) but also rapid recovery under rest (G' : 35 KPa; G'' : 9.6 KPa), which was reproducible in subsequent strain cycles. This viscoelastic behaviour explains the recovery of pressure when the plunger stopped the downward movement, and also the larger pressure required for the retraction.

3.3. Use of the sensor while printing

Based on the results obtained in the characterization of the masses, 30 printlets (8.20 mm diameter \times 4.10 mm height) were printed using the paste-like formulation containing isoleucine and using some of the parameters determined as optimal for this formulation: flow rate 48.07 mm³/s (high printing speed), printing temperature at 37 °C, and internal nozzle diameter of 0.84 mm.

Using the data logger incorporated in the M3DIMAKER 3D printing platform, the applied pressure values of the 3D printhead with Laguna SSE printhead were collected and it was possible to verify how the process was kept under control during almost the entire production of the printlets. In the first printlet produced, a non-homogeneous applied pressure was observed (Fig. 10), which coincided with a non-viable pharmaceutical form (Fig. 10D) without adequate final quality attributes (CQA). Subsequently, the process remained under control since the pressure remained constant (\approx 100 kPa) during the printing of subsequent dosage forms up to printlet number 18. During the printing of the 18th printlet, a notably higher applied pressure value was recorded

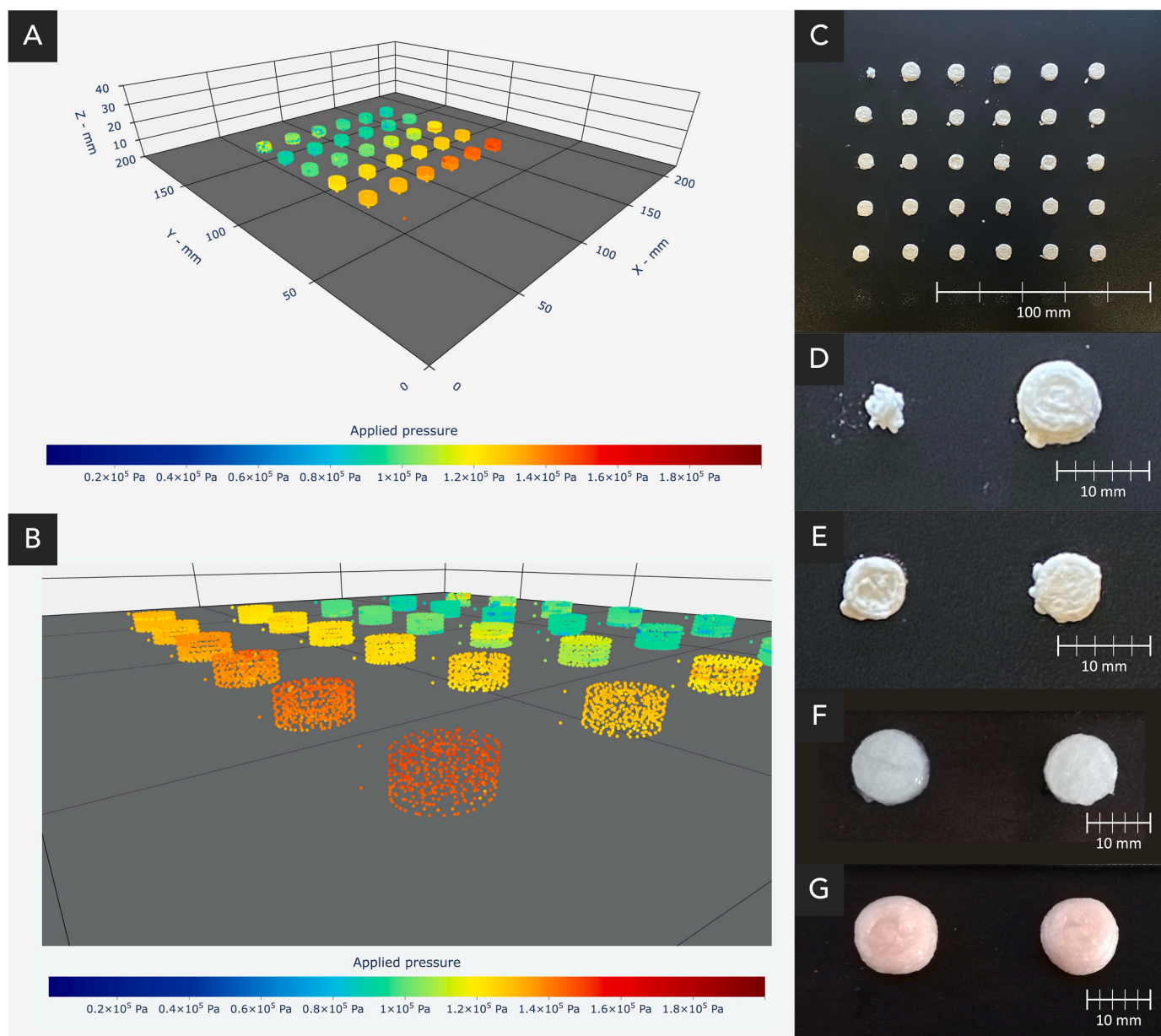


Fig. 10. A. General view of the applied pressure 3D scatter (paste-like formulation). B. Lateral view of the applied pressure 3D scatter (paste-like formulation). C. General picture of the 30 printlet batch (paste-like formulation). D. Detailed view of the 1st (left) and 2nd (right) printlet (paste-like formulation). E. Detailed view of the 17th (left) and 18th printlet (right) (paste-like formulation). F. Detailed view of two printlets (vaseline). G. Detailed view of two printlets (gel-like formulation).

for a layer, coinciding with the obstruction of the nozzle. This subsequently manifested as a defect in the perimeter of the printlet, as shown in Fig. 10E. This higher value was maintained consistently during the remaining processing of the batch without an upward trend indicating a complete blockage. The 3D scatter plots of the pressures made it possible to visually establish which prints were made with the desired pressure and which were not. As can be seen in Fig. 10A-B, this parameter is closely related to the final quality attributes (CQA) of the final dosage forms.

4. Conclusions

A pressure sensor has been employed for the first time inside an SSE pharmaceutical 3D printer as a PAT tool. The sensor was suitable for the successful characterization of different masses, such as soft vaseline with temperature-dependent flow properties, gel-like masses with plastic behaviour or paste-like masses with predominantly viscoelastic

behaviour, using the conditions to be employed in the 3D printing process. It was possible to identify the most suitable printing conditions for the different semi-solid masses. For the gel-like mass, the best printing temperature was found to be 60 °C, using a larger internal diameter nozzle (1.60 mm) and high printing speeds (high flow rate 48.07 mm³/s). For the paste-like mass, several sets of parameters were found to lead to good printing results, using temperatures between 37 °C and 60 °C regardless of the internal diameter of the nozzle (1.60 mm or even 0.84 mm), although using high flow rates (48.07 mm³/s). Therefore, control of critical feedstock material attributes and 3D printing process parameters, such as printing speed, inner nozzle diameter or extruder temperature, may enable a high-fidelity 3D printing process for the future of personalized medicine.

CRediT authorship contribution statement

Eduardo Díaz-Torres: Conceptualization, Data curation, Formal

analysis, Investigation, Methodology, Writing – original draft, Writing – review & editing. **Lucía Rodríguez-Pombo**: Data curation, Formal analysis, Writing – review & editing. **Jun Jie Ong**: Data curation, Formal analysis, Writing – review & editing. **Abdul W. Basit**: Supervision, Resources, Writing – review & editing. **Ana Santoveña-Estévez**: Supervision, Resources, Writing – review & editing. **José B. Fariña**: Supervision, Resources, Writing – review & editing. **Carmen Alvarez-Lorenzo**: Conceptualization, Data curation, Methodology, Supervision, Writing – review & editing. **Alvaro Goyanes**: Conceptualization, Methodology, Project administration, Resources, Supervision, Writing – review & editing.

Declaration of Competing Interest

The authors declare that they have no known competing financial interests or personal relationships that could have appeared to influence the work reported in this paper.

Data availability

Data will be made available on request.

Acknowledgements

E.D.T. would like to acknowledge support from the pre-doctoral training programme for research personnel in the Canary Islands of the Consejería de Economía, Conocimiento y Empleo, 85% co-financed by the European Social Fund (ESF), within the framework of the ESF Operational Programme for the Canary Islands 2014-2020 (grant number: TESIS2020010087. LRP acknowledges the predoctoral fellowship provided by the Ministerio de Universidades [Formación de Profesorado Universitario (FPU 2020)].

References

- Barry, B.W., Grace, A.J., 1971. Rheological properties of white soft paraffin. *Rheol. Acta* 10, 113–120.
- Borre, E., Stumbé, J.-F., Bellemin-Lapponnaz, S., Mauro, M., 2015. Light-Powered Self-Healable Metallosupramolecular Soft Actuators. *Angew. Chem. Int. Ed.* 55, 1313–1317.
- Conceicao, J., Farto-Vaamonde, X., Goyanes, A., Adeoye, O., Concheiro, A., Cabral-Marques, H., Sousa Lobo, J.M., Alvarez-Lorenzo, C., 2019. Hydroxypropyl-beta-cyclodextrin-based fast dissolving carbamazepine printlets prepared by semisolid extrusion 3D printing. *Carbohydr. Polym.* 221, 55–62.
- Crişan, A.G., Iurian, S., Porfire, A., Rus, L.M., Bogdan, C., Casian, T., Lucacel, R.C., Turza, A., Porav, S., Tomuța, I., 2022. QbD guided development of immediate release FDM-3D printed tablets with customizable API doses. *Int. J. Pharm.* 613, 121411.
- Díaz-Torres, E., Santoveña, A., Fariña, J., 2021. A micro-extrusion 3D printing platform for fabrication of orodispersible printlets for pediatric use. *Int. J. Pharm.* 605, 120854.
- Europe, C.o., 2021a. <5.25> Process analytical technology, European Pharmacopoeia (Ph. Eur.), 10th ed. Council of Europe.
- Europe, C.o., 2021b. <5.28> Multivariate statistical process control, European Pharmacopoeia (Ph. Eur.), 10th ed. Council of Europe.
- Fang, D., Yang, Y., Cui, M., Pan, H., Wang, L., Li, P., Wu, W., Qiao, S., Pan, W., 2021. Three-Dimensional (3D)-Printed Zero-Order Released Platform: a Novel Method of Personalized Dosage Form Design and Manufacturing. *AAPS PharmSciTech* 22, 37.
- Govender, R., Eric, K., Larsson, A., Tho, I., 2021. Polymers in Pharmaceutical Additive Manufacturing: a Balancing Act between Printability and Product Performance. *Adv. Drug Deliv. Rev.* 177, 113923.
- Goyanes, A., Madla, C.M., Umerji, A., Duran Pineiro, G., Giraldez Montero, J.M., Lamas Diaz, M.J., Gonzalez Barcia, M., Taherali, F., Sanchez-Pintos, P., Couce, M.L., Gaisford, S., Basit, A.W., 2019. Automated therapy preparation of isoleucine formulations using 3D printing for the treatment of MSUD: first single-Centre, prospective, crossover study in patients. *Int. J. Pharm.* 567, 118497.
- Gudeman, J., Jozwiakowski, M., Chollet, J., Randell, M., 2013. Potential risks of pharmacy compounding. *Drugs in R&D* 13, 1–8.
- Johannesson, J., Khan, J., Hubert, M., Teleki, A., Bergström, C.A.S., 2021. 3D-printing of solid lipid tablets from emulsion gels. *Int. J. Pharm.* 597, 120304.
- Melocchi, A., Briatico-Vangosa, F., Uboldi, M., Parietti, F., Turchi, M., von Zeppelin, D., Maroni, A., Zema, L., Gazzaniga, A., Zidan, A., 2021. Quality considerations on the pharmaceutical applications of fused deposition modeling 3D printing. *Int. J. Pharm.* 592, 119901.
- MHRA, 2022. Consultation on Point of Care Manufacturing. UK Government, United Kingdom.
- Ozolat, I.T., 2016. 3D Bioprinting: Fundamentals, Principles and Applications, 1st ed. Elsevier.
- Ozolat, I.T., Hospodiuk, M., 2016. Current advances and future perspectives in extrusion-based bioprinting. *Biomaterials* 76, 321–343.
- Rahman, J., Quodbach, J., 2021. Versatility on demand - the case for semi-solid micro-extrusion in pharmaceuticals. *Adv. Drug Deliv. Rev.* 172, 104–126.
- Rahman, M., Almalki, W.H., Alghamdi, S., Alharbi, K.S., Khalilullah, H., Habban Akhter, M., Keshari, A.K., Sharma, N., Singh, T., Soni, K., Hafeez, A., Beg, S., 2021. Three 'D's: Design approach, dimensional printing, and drug delivery systems as promising tools in healthcare applications. *Drug Discov* 26, 2726–2733.
- Seoane-Viño, I., Gómez-Lado, N., Lázare-Iglesias, H., García-Otero, X., Antúnez-López, J.R., Ruibal, Á., Varela-Correa, J.J., Aguiar, P., Basit, A.W., Otero-Espinar, F. J., González-Barcia, M., Goyanes, A., Luzardo-Álvarez, A., Fernández-Ferreiro, A., 2020a. 3D Printed Tacrolimus Rectal Formulations Ameliorate Colitis in an Experimental Animal Model of Inflammatory Bowel Disease. *Biomedicines* 8, 563.
- Seoane-Viño, I., Ong, J.J., Luzardo-Álvarez, A., González-Barcia, M., Basit, A.W., Otero-Espinar, F.J., Goyanes, A., 2020b. 3D printed tacrolimus suppositories for the treatment of ulcerative colitis. *Asian Journal of Pharmaceutical Sciences*. 16 (1), 110–119.
- Seoane-Viño, I., Trenfield, S.J., Basit, A.W., Goyanes, A., 2021a. Translating 3D printed pharmaceuticals: from hype to real-world clinical applications. *Adv. Drug Deliv. Rev.* 174, 553–575.
- Seoane-Viño, I., Januskaite, P., Alvarez-Lorenzo, C., Basit, A.W., Goyanes, A., 2021b. Semi-solid extrusion 3D printing in drug delivery and biomedicine: Personalised solutions for healthcare challenges. *J. Control. Release* 332, 367–389.
- Tagami, T., Ito, E., Kida, R., Hirose, K., Noda, T., Ozeki, T., 2021. 3D printing of gummy drug formulations composed of gelatin and an HPMC-based hydrogel for pediatric use. *Int. J. Pharm.* 594, 120118.
- Trenfield, S.J., Tan, H.X., Goyanes, A., Wilsdon, D., Rowland, M., Gaisford, S., Basit, A. W., 2020. Non-destructive dose verification of two drugs within 3D printed polyprintlets. *Int. J. Pharm.* 577, 119066.
- Vithani, K., Goyanes, A., Jannin, V., Basit, A.W., Gaisford, S., Boyd, B.J., 2019. A Proof of Concept for 3D Printing of Solid Lipid-based Formulations of Poorly Water-Soluble Drugs to Control Formulation Dispersion Kinetics. *Pharm. Res.* 36, 102.
- Watson, C.J., Whitley, J.D., Siani, A.M., Burns, M.M., 2021. Pharmaceutical compounding: a history, Regulatory Overview, and Systematic Review of compounding Errors. *J. Med. Toxicol.* 17, 197–217.
- Yan, T.-T., Lv, Z.-F., Tian, P., Lin, M.-M., Lin, W., Huang, S.-Y., Chen, Y.-Z., 2020. Semi-solid extrusion 3D printing ODFs: an individual drug delivery system for small scale pharmacy. *Drug Dev. Ind. Pharm.* 46, 531–538.
- Yu, L.X., Amidon, G., Khan, M.A., Hoag, S.W., Polli, J., Raju, G.K., Woodcock, J., 2014. Understanding Pharmaceutical Quality by Design. *AAPS Journal* 16, 771–783.
- Zhang, L., Mao, S., 2017. Application of quality by design in the current drug development. *Asian J. Pharm. Sci* 12, 1–8.
- Zhang, M., Vora, A., Han, W., Wojtecki, R.J., Maune, H., Le, A.B.A., Thompson, L.E., McClelland, G.M., Ribet, F., Engler, A.C., Nelson, A., 2015. Dual-Responsive Hydrogels for Direct-Write 3D Printing. *Macromolecules* 48, 6482–6488.
- Zhang, J., Thakkar, R., Zhang, Y., Maniruzzaman, M., 2020. Structure-function correlation and personalized 3D printed tablets using a quality by design (QbD) approach. *Int. J. Pharm.* 590, 119945.
- Zidan, A., Alayoubi, A., Asfari, S., Coburn, J., Ghamraoui, B., Cruz, C., Ashraf, M., 2018a. Development of mechanistic models to identify critical formulation and process variables of pastes for 3D printing of modified release tablets. *Int. J. Pharm.* 555.
- Zidan, A., Alayoubi, A., Coburn, J., Asfari, S., Ghamraoui, B., Cruz, C., Ashraf, M., 2018b. Extrudability analysis of drug loaded pastes for 3D printing of modified release tablets. *Int. J. Pharm.* 554.